

Reprocessing of UV-weathered wood flour reinforced polypropylene composites: Study of a natural outdoor exposure

L. Soccalingame, Perrin Didier, J.-C. Bénézet, Anne Bergeret

▶ **To cite this version:**

L. Soccalingame, Perrin Didier, J.-C. Bénézet, Anne Bergeret. Reprocessing of UV-weathered wood flour reinforced polypropylene composites: Study of a natural outdoor exposure. Polymer Degradation and Stability, 2016, 133, pp.389-398. 10.1016/j.polymdegradstab.2016.09.011 . hal-02900366

HAL Id: hal-02900366

https://imt-mines-ales.hal.science/hal-02900366

Submitted on 10 Jun 2021

HAL is a multi-disciplinary open access archive for the deposit and dissemination of scientific research documents, whether they are published or not. The documents may come from teaching and research institutions in France or abroad, or from public or private research centers.

L'archive ouverte pluridisciplinaire **HAL**, est destinée au dépôt et à la diffusion de documents scientifiques de niveau recherche, publiés ou non, émanant des établissements d'enseignement et de recherche français ou étrangers, des laboratoires publics ou privés.

Reprocessing of UV-weathered wood flour reinforced polypropylene composites: Study of a natural outdoor exposure

L. Soccalingame, D. Perrin, J.-C. Bénézet, A. Bergeret*

C2MA, Ecole des Mines d'Alès, 6 Avenue de Clavières, 30319, Alès Cedex, France[1]

A B S T R A C T

This work aims to determine and understand the influence of a one-year natural UV weathering on the reprocessing of a wood-plastic composite (WPC), i.e. a wood flour reinforced polypropylene (PP) composites. Two wood flour contents (10% w/w and 30% w/w) were studied in comparison to neat PP. Injected samples of were submitted to a long-term natural outdoor exposure followed by one complete reprocessing cycle (grinding then injection). The visual aspect evolution of the surface was followed by optical microscopy. In order to understand the material physical degradation, the mechanical behaviour was measured thanks to tensile and Charpy impact tests. The assessment of the microstructural evolution was performed by differential scanning calorimetry (crystallinity ratio), rheological tests (viscosity), size exclusion chromatography tests (average molecular weights) and infrared spectroscopy analysis (chemical structure). A "regeneration" phenomenon was highlighted as mechanical properties are recovered after reprocessing. This is due to the mixing and the dilution of the degraded chains into the material as no recombination or crosslinking mechanism was detected. A comparison with an artificial UV weathering performed on the same samples and exposed in a previous study was finally investigated.

Keywords:
Polypropylene
Wood flour
Biocomposites
Reprocessing
Natural UV weathering
Microstructure
Mechanical properties
Degradation

1. Introduction

The wood-plastic composites (WPCs) mainly concern thermoplastic polymers reinforced by wood fibres or flour and are widespread in outdoor decking applications. The most common polymer matrices are polypropylene (PP), polyethylene (PE) and polyvinyl chloride (PVC). With the growing use of WPC, their end-of-life issue is expected to become larger and increasingly difficult and expensive. Assessing WPC recycling capability is up to now a challenging economic and scientific goal.

Several previous studies investigated the reprocessing of WPC or natural fibre reinforced composites. Positive results were found as satisfactory properties and a good aptness to be recycled were observed [1–3]. Despite these favourable tendencies in results, thermal degradation was found to be the major issue in WPC reprocessing. Indeed, many studies showed that polymer matrices tend to degrade by chain scissions under severe thermal and stress cycles [3–12]. Vegetal fibers or flours are also prone to degrade under these conditions: decreases in particle size and particle rigidity as well as chemical attrition were consensually reported [3], [13–16].

A major degradation factor during the life cycle of WPCs is outdoor exposure which is mainly characterized by a combined UV/humidity exposure. Weathering performed on WPCs generally induced a mechanical property alteration, a surface erosion with flouring effect, a surface yellowing and bleaching, a surface cracking, crystallinity changes and a dimensional instability (swelling and shrinking) [17–19]. Concerning the PP matrix degradation in WPCs, weathering degradation generally consists in an oxidation phenomenon leading to the formation of radicals in the polymer [20]. This results in chain scissions decreasing the polymer chain length and entanglement, which deteriorates mechanical and rheological properties of the composite. Furthermore, the oxidation of PP leads to carbonyl and hydroxyl groups which are polar groups. It was noticed that these polar groups improve compatibility between polar fillers such as lignocellulosic fibres, bettering interface between untreated natural fibres and polymer matrix [20]. Concerning the vegetal fillers, lignin bleaching and particle swelling were evidenced as the main sources of material

* Corresponding author.
E-mail address: Anne.Bergeret@mines-ales.fr (A. Bergeret).

[1] C2MA is a member of the European Polysaccharide Network of Excellence (EPNOE), www.epnoe.eu.

degradation [17,21]. However, Peng et al. highlighted the antioxidant role of lignin as it prevents mechanical property degradation. On the contrary, cellulose does not bleach but impacts more importantly mechanical properties when degrading [22,23]. Otherwise, stabilizing solutions exist and are common in polymers such as hindered amine light stabilizers (HALS) or UV absorbers [24].

Few studies deal with the reprocessing of weathered polymer and composite materials. Jansson et al. [25] studied the reprocessing of oxidised post-consumer PP/PE copolymers. They found that the elongation drops considerably after each ageing step and returns approximately to the initial value after each extrusion cycle. Three combined mechanisms were proposed: i) changes in the crystallinity ratio, ii) degradation located at the surface and iii) dilution of degraded polymer chains after re-extrusion. Besides, a synergistic effect between extrusion and ageing was evidenced as the combination degrades stronger than reprocessing or ageing does separately. Luzuriaga et al. [26] use a similar methodology with various polymers and an accelerated UV weathering. They showed that the PP melt flow index (MFI) increases progressively with reprocessing cycles combined with UV ageing. This PP viscosity evolution indicates a chain scission occurring during both ageing and reprocessing without the shorter polymer chains being diluted. Afterwards, a similar conclusion were expressed by both Jansson et al. [25] and Luzuriaga et al. [26]: these authors add that a complete understanding of the results remains elusive as the amount and the type of stabilizing additives contained in commercialised polymer granules are usually unknown. Concerning the reprocessing of weathered PP based WPCs, our previous work [19] highlighted the same trends than Jansson et al. [25] with the recovering of mechanical properties after reprocessing of artificially UV weathered samples. Numerous technics were used to understand this “regeneration” phenomenon: SEC measurements, rheological and DMTA tests evidenced that the reprocessing allows the degraded chains and the non-degraded ones to be mixed together at the molten state to obtain a homogenized material. A PP matrix recombination also occurs as the chain length increases and the carbonyl concentration decreases after reprocessing [19].

To consolidate those conclusions about the reprocessing behaviour of weathered WPCs, this work aims to determine and understand the influence of a one-year natural UV weathering on the reprocessing of PP based WPCs. A comparison with an artificial UV weathering on similar materials is proposed to determine if tendencies are in accordance between both UV weathering. Injected neat PP and PP/wood flour (10%w and 30%w wood content) were submitted to a natural outdoor exposure followed by a reprocessing cycle (grinding and injection). The evolution in surface visual aspects was followed by optical microscopy. The mechanical behaviour was measured thanks to tensile and Charpy impact tests to understand the material physical degradation. Differential scanning calorimetry (crystallinity ratio), rheological tests (viscosity), size exclusion chromatography (average molecular weights) tests and infrared spectroscopy (chemical structure) were performed to assess the microstructural evolution.

2. Materials & methods

2.1. Raw materials

Polypropylene (PP) used in this study is a standard homopolymer PP H733-07 grade supplied by Braskem Co. (Brazil) with a melt flow rate of 7.5 g/10min (230 °C, 2.16 kg) according to ISO 1133 standard. Maleic anhydride grafted polypropylene (MAPP) with a 1%w/w grafting rate is used as coupling agent and provided by Arkema Co. (France) under the trademark Orevac® CA100. It was dry-mixed before processing at 3%w/w of the PP. The wood flour is based on spruce wood with a particle size included in the 200 μm−500 μm range and is obtained from AFT Plasturgie Co. (France). The wood flour was added at 10%w/w and 30%w/w in the PP/MAPP matrix.

2.2. Processes and natural weathering

The processing methodology is summarized in Fig. 1 and the successive stages are detailed below.

Beforehand, the wood flour is dried 15 h at 80 °C to remove moisture from the particles. Then, the PP matrix and the wood particles are mixed together in a BC21 Clextral (France) co-rotating twin-screw extruder (step ①). Its L/d ratio is 36 with a 25 mm screw diameter and a 900 mm screw length. Temperature is set at 180 °C along the barrel. The screw speed is fixed at 300 rpm with a total feeding rate of 4 kg/h. The extruder is equipped with a 4 mm die diameter. The extruded compound rods are cooled into water and granulated. Pellets are kept 6 h at 80 °C (step ②) in an air-pulsing apparatus.

The pellets are injection moulded to produce normalized samples on a Krauss-Maffei KM50-T180CX. The temperature is fixed at 210 °C along the barrel. The mould is kept at 25 °C by a water cooling system. The plasticization and injection speed are set respectively at 120 rpm and 60 $cm^3\ s^{-1}$. The samples are injected to obtain dog-bone samples 1A according to ISO 527-2 (step ③). Samples are characterized at this step to evaluate their initial stage (INIT).

ISO 1A samples are exposed according to EN ISO 877 standard in natural site in the South of France on galvanized steel racks (step ④). The exposure started in June 2012 and finished in June 2013 and included climatic conditions from the four annual seasons. According to the mentioned standard, the samples are fixed on the racks at an angle of 45° with the ground on a south facing flat land (Fig. 2).

Aged samples are characterized (NAT stage), then grinded and injected to simulate recycling (step ⑤). The grinding process is performed in a RETSCH SM300 cutter mill to obtain flakes. The grinding process is carried out at 700 rpm at room temperature with an 8 mm sieve. The flakes are stored at room temperature and vacuum dried overnight at 80 °C before injection moulding (REP stage).

Samples used in this study are detailed in Table 1.

2.3. Characterization of surface aspect evolution

Colour and texture changes of the sample surface are visually assessed with a Leica WILD M10 optical microscope. Pictures are taken at ×10 and ×50 magnifications with a Leica DFC 420 camera. Pictures from a same material are taken with the same light intensity to properly discern colour changes.

2.4. Mechanical characterization

2.4.1. Tensile tests

Classical tensile tests are performed on a Zwick Z010 apparatus with a 10 kN load cell. These tests are performed according to the ISO 527 standard. The crosshead speed is set at 50 mm/min for the break property measurements. Five measurements are carried out for strength and elongation at break measurements.

2.4.2. Charpy tests

Impact strength is measured with a Charpy pendulum impact tester ZWICK 5102. The tests are performed according to the ISO 179 standard and repeated for ten unnotched samples. A 4 J

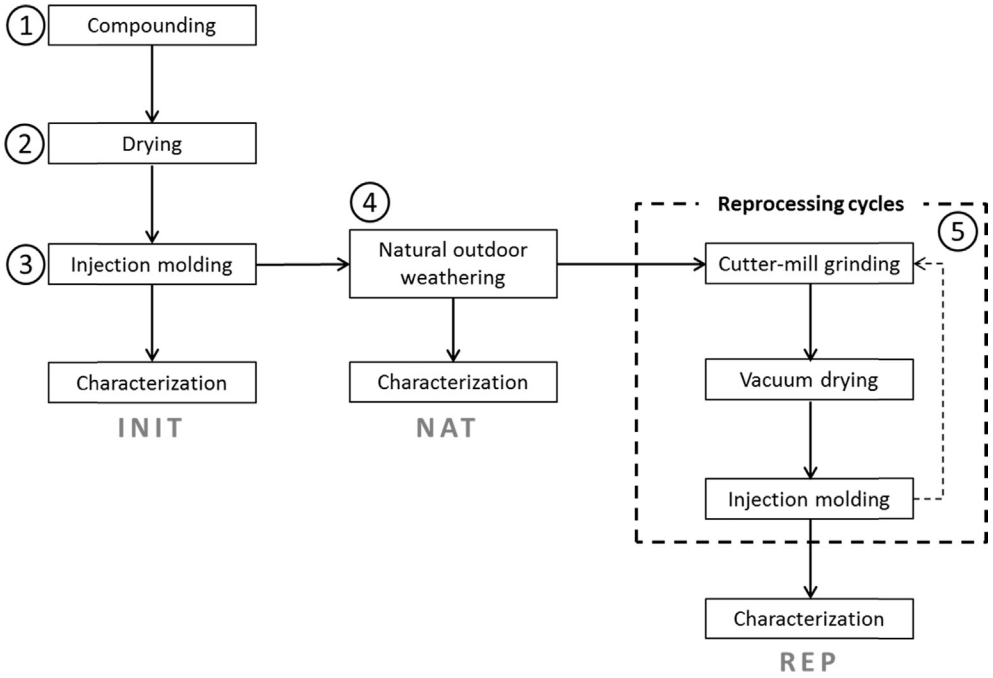


Fig. 1. Stages of the weathering and reprocessing stages.

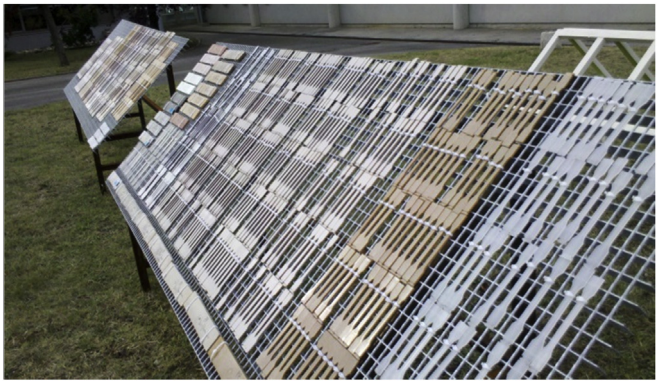


Fig. 2. Exposure racks used in this study.

pendulum is chosen. The unnotched samples are sawn from the ISO 1A injected samples with 80 × 10 × 4 mm^3 dimensions.

2.5. Characterization of the polymer microstructure

2.5.1. Differential scanning calorimetry (DSC)

The melting and crystallisation behaviours of biocomposites and neat polymer are assessed through differential scanning calorimetry (DSC) using a Perkin Elmer apparatus (Pyris Diamond) equipped with a cooling attachment, under a nitrogen atmosphere. Two heating steps interspersed with a cooling step from 30 °C to 220 °C at a constant rate of 10 °C.min^{-1} are carried out. The sample weights are approximately 10 mg. They are analyzed in standard aluminium DSC pans. At least, two specimens are used for each test to ensure reproducibility. Melting enthalpies are obtained from the 1st and the 2nd heating step. The intermediate cooling step was conducted at 10 °C.min^{-1}. The crystallinity χ_c is calculated according to (Equation (1)):

$$\chi c = \frac{\Delta Hm}{W \times \Delta Hm100\%} \times 100 \quad (1)$$

where ΔHm is the melting enthalpy of the composite, W is the PP content by weight in the composite and ΔHm100% is the melting enthalpy for a 100% crystalline PP polymer. It is considered equal to 209 J/g [27].

2.5.2. Rheological tests

The evolution of the rheological material properties directly reflects changes in molecular parameters such as the chain scission and crosslinking phenomena. Thus, dynamic rheological measurements are carried out to assess the change in complex viscosity using an ARES rheometer (Rheometric Scientific). The melt viscoelasticity tests in oscillatory shear mode are performed with parallel plate equipment at a fixed temperature of 180 °C. The plate diameter is 25 mm and the gap between them is 1 mm. A frequency sweep is carried out from 0.1 to 100 rad s^{-1} for each experiment.

The samples are cut at the extremities of the injected dog-bone samples and placed between the parallel plates. Once the fixed temperature is reached, the gap is controlled at 1 mm. Then, the molten excessive matter is removed and the test is started. At least

Table 1
Designation of the studied materials.

Wood flour content by weight	Unaged INITial state	NATural UV aged	REProcessed after natural UV ageing
0%	PP_{INIT}	PP_{NAT}	PP_{REP}
10%	$PP/WF10_{INIT}$	$PP/WF10_{NAT}$	$PP/WF10_{REP}$
30%	$PP/WF30_{INIT}$	$PP/WF30_{NAT}$	$PP/WF30_{REP}$

three tests are performed for each material.

Additionaly, to determine information about the polymer microstructure at the molten state, the Cole-Cole model was used. The Cole-Cole diagram representation consists in plotting the imaginary part η"of the complex viscosity η^* as a function of its real counterpart η'. If the studied polymeric material obeys the Cole-Cole model, plotted data form a circular arc described as follow (Equation (2)) [28]:

$$\boldsymbol{\eta}^*(\boldsymbol{i\omega}) = \frac{\boldsymbol{\eta}_0}{1 + (\boldsymbol{i\omega\lambda})^{(1-\alpha)}} \tag{2}$$

where ω is the test pulsation, λ is the macromolecular chain relaxation time, α is the dispersion parameter and η_0 is the newtonian viscosity. Thus, the complex viscosity and the concomittant molecular motions are dependent on frequency for the mechanical relaxation of stress. The real and imaginary part of the complex viscosity as modeled by the Cole-Cole function can be derived from these two following Havriliak and Negami equations (Equations (3) and (4)) [29]:

$$\boldsymbol{\eta}'(\boldsymbol{\omega}) = \frac{\boldsymbol{\eta}_0(1 + (\boldsymbol{\omega\lambda})^{(1-\alpha)}\boldsymbol{sin}\left(\frac{\alpha\pi}{2}\right)}{1 + 2(\boldsymbol{\omega\lambda})^{(1-\alpha)}\boldsymbol{sin}\left(\frac{\alpha\pi}{2}\right) + (\boldsymbol{\omega\lambda})^{2(1-\alpha)}} \tag{3}$$

$$\boldsymbol{\eta}''(\boldsymbol{\omega}) = \frac{\boldsymbol{\eta}_0(\boldsymbol{\omega\lambda}_0)^{(1-\alpha)}\cos\left(\boldsymbol{\alpha}\frac{\pi}{2}\right)}{1 + 2(\boldsymbol{\omega}0_{\boldsymbol{\lambda}})^{(1-\alpha)}\sin\left(\boldsymbol{\alpha}\frac{\pi}{2}\right) + (\boldsymbol{\omega\lambda}_0)^{2(1-\alpha)}} \tag{4}$$

By fitting these two equations with experimental data at each test frequency by a least-square procedure, one can determine the relaxation time λ, the dispersion parameter α and the newtonian viscosity η_0 by extrapolation to low frequencies. These three parameters are representative of the polymer mobility and the polymer chain length above melting temperature.

2.5.3. Size exclusion chromatography (SEC)

The evolution of average molecular weights (in number $\overline{Mn}$ and in weight $\overline{Mw}$) of PP in neat PP and PP/WF composites is studied to evaluate the effect of successive processing cycles on the PP degradation. Size-exclusion chromatography is performed by Catalyse Co. (Marseille, France). Fragments are cut into the middle part of the dog-bone injected samples and solubilized into 1,2,4-trichlorobenzene (TCB) at a concentration of 3 mg mL^{-1}. These solutions are agitated at 150 °C and, then filtered before test. The separation is carried out by using a pre-column PLgel Olexis Guard 7.5 × 50 mm and three PLgel Olexis Guard 7.5 × 300 mm columns. The temperature is set at 150 °C, and the flow rate is 1 mL min^{-1}. The solvent is 1,2,4-trichlorobenzene (TCB) with 0.2 $mg.L^{-1}$ of butylhydroxytoluol (BHT) added to stabilize the polymer against oxidative degradation. Sample fragments were cut on the exposed face and the unexposed face for comparison. Two tests were performed for each sample.

2.5.4. Infrared spectroscopy

Infrared spectroscopy is carried out to assess the evolution of specific chemical groups during the degradation phenomenon induced by weathering and reprocessing. A spectrometer IFS66 from Bruker® is used in ATR mode (Attenuated Total Reflectance). The spectra are measured from 400 cm^{-1} to 4000 cm^{-1} with a 2 cm^{-1} resolution on the sample exposed surface. The mentioned peaks were normalized with the 2912 cm^{-1} attributed to a C—H stretching band of methyl groups CH_3. This band is chosen as a reference because it changed minimally during weathering [30].

3. Results and discussion

Results of this present study will be compared with our previous study results concerning an artificial weathering [19]. Discrepancies between initial state values are due to different processing conditions between these two studies.

3.1. Evolution of the surface aspect

The sample surface aspect is presented in Table 2 for PP, PP/WF10 and PP/WF30 respectively as a function of the different stages (INIT, NAT and REP). Neat PP surfaces exhibit more important cracking phenomena due to photodegradation during outdoor weathering (NAT step) than during artificial UV weathering [19]. Moreover, the reprocessing step leads to a material displaying a strong yellowing effect. For both PP/WF10 and PP/WF30, outdoor weathering induces a wood particle bleaching and a protrusion of these particles at the surface with many cracks into the PP matrix as for artificial weathering. This degradation is so important that a flouring phenomenon is obtained on the exposed surface. The bleaching leads to an entirely white surface with no brown parts visible. The surface is whiter than in the case of artificial weathering [19]. It was previously shown that this wood bleaching is well-known and is mainly due to the lignin chromophoric groups absorbing in the UV/visible region. This photo-degradation is explained by two competing reactions in the literature [31,32]: the first one is lignin oxidation, which leads to the formation of para-quinone chromophoric structures, and the second one involves reduction of the paraquinone structures to hydroquinones, which leads to photo-bleaching. Moreover, some black particles are visible as aggregates accumulated into the cracks. These black aggregates are supposed to be airborne pollutants such as combustion residues from industrial or domestic activities or emissions from road transport in the surrounding area of the natural ageing site.

Then, after reprocessing, the surfaces recover a glossy aspect thanks to injection moulding process with no protrusion of the wood particles. The bleached aspect has disappeared but the global colour is much darker than the initial state. Similar phenomena were observed in the case of UV artificial ageing [19]. This is probably induced to a combined effect of the mixing and dilution of bleached parts and the darkening due to wood degradation during process.

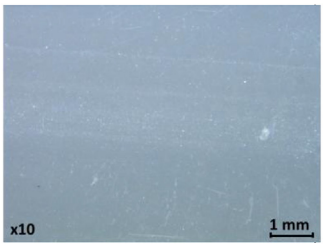
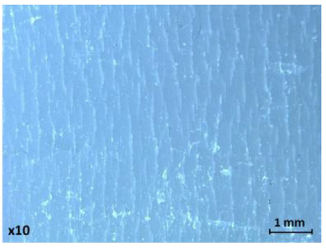
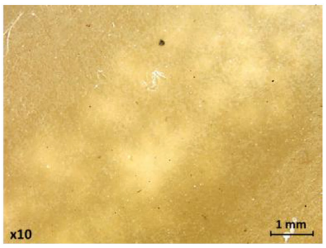
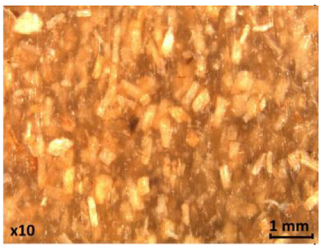
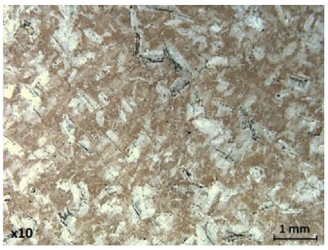
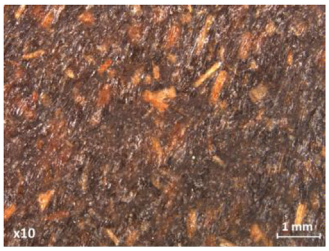
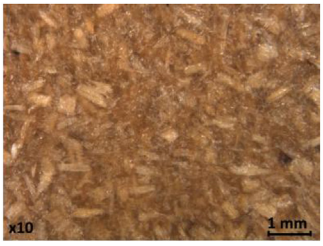
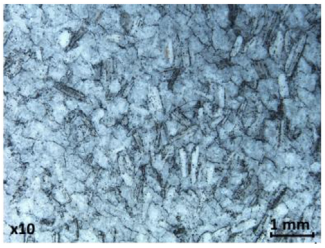
3.2. Evolution of mechanical behaviour

3.2.1. Tensile property variations

Fig. 3 shows tensile ultimate strength values for all studied materials at each stage (INIT, NAT, REP). A drastic decrease in the yield strength with the natural weathering was observed with loss of 60%, 18% and 14% for PP, PP/WF10 and PP/WF30 respectively. This can be ascribed to a chain scission mechanism by photo-degradation. Then, the reprocessing step after natural weathering brings strength values up. PP, PP/WF10 and PP/WF30 recover 82%, 97% and 100% respectively of their initial strength. If comparing with artificial weathering, previous results showed no significant degradation of yield strength for similar materials [19]. Thus, the natural exposure is more detrimental than the artificial ones under these conditions.

Concerning the tensile elongation at yield (Fig. 4), the addition of wood flour globally decreases the deformation rate because the PP chain mobility is restrained by wood particles. Neat PP exhibits a large drop from 7% ± 0.3%−1% ± 0.2% due to chain scission but recovers little ductility after reprocessing (4% ± 1.7%). Concerning the PP/WF composites, no significant variation of the elongation was observed after weathering and reprocessing. PP/WF materials are

Table 2
Micrographs of sample surface for neat PP and PP/WF composites at the different stages: INIT, NAT and REP.

	INIT	NAT	REP
Neat PP			
PP/WF10			
PP/WF30			

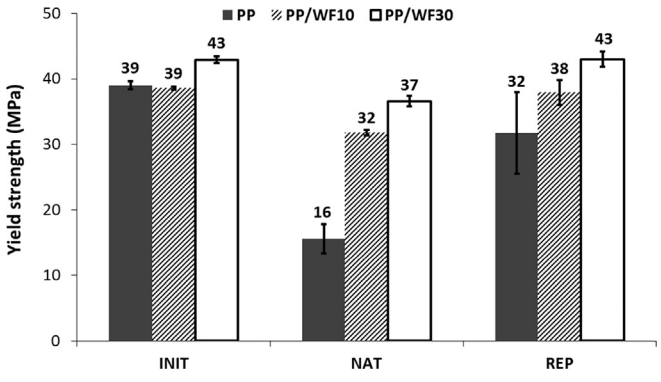


Fig. 3. Tensile yield strength of PP and PP/WF composites at the initial state (INIT), at the weathered state (NAT), at the reprocessed state after weathering (REP).

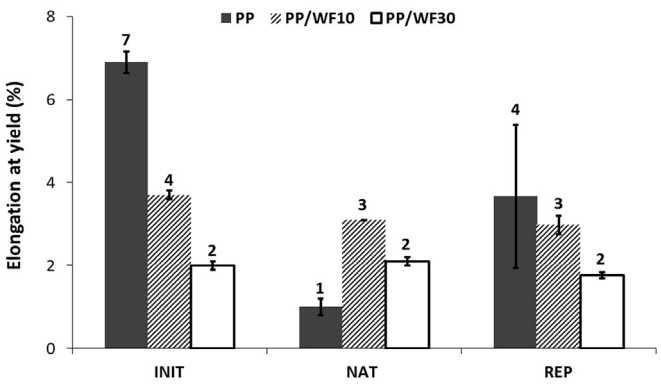


Fig. 4. Tensile elongation at yield of PP and PP/WF composites at the initial state (INIT), at the weathered state (NAT), at the reprocessed state after weathering (REP).

the most stable against weathering and reprocessing as their evolution is very low compared to neat PP. The addition of wood flour seems to stabilize the PP polymer against degradation. This observation is in accordance with conclusions from Peng et al. stating that high wood content leads to high amount of lignin which has an antioxidant role and hinders mechanical degradation [22,23]. In the case of artificial weathering, neat PP is less degraded (4% ± 0.1%) and recovers better its value of 8% ± 0.1% in elongation after reprocessing. The PP/WF composite elongations stay in the same range and are not impacted by the artificial weathering. The similar tendency of tensile property recovery after reprocessing was observed only for artificially weathered PP samples, PP/WF composites being lowly impacted by weathering and reprocessing [19].

3.2.2. *Impact strength variations*

Results from un-notched Charpy tests are plotted in Fig. 5. No break for neat PP is observed at the initial state thanks to its ductile property. PP becomes brittle after the natural weathering step with very low impact strength (1 ± 0.1 kJ/m^2) but return to its ductile state (25 ± 3.9 kJ/m^2) after reprocessing. This high impact strength value confirms the tendency found with tensile elongation after reprocessing. Concerning PP/WF10 and PP/WF30, the same tendency is observed with a drop after weathering, and "regeneration" of impact properties after reprocessing. This phenomenon is less significant for PP/WF30 probably due to the stabilizing effect of lignin [22,23].

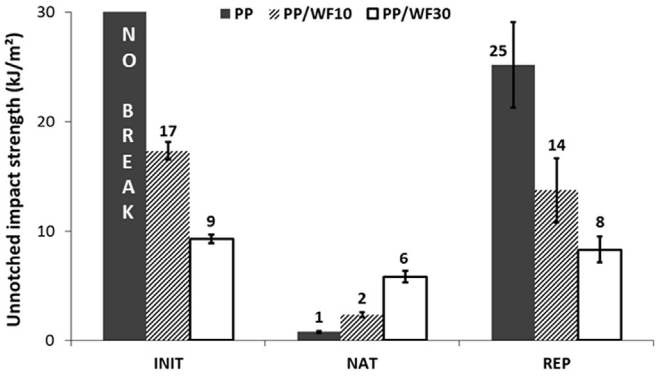


Fig. 5. Un-notched impact strength by Charpy tests at the initial state (INIT), at the weathered state (NAT), at the reprocessed state after weathering (REP).

Table 3
Crystallinity percentages of PP/WF composites measured by DSC tests at the initial state (INIT), at the naturally weathered state (NAT) and at the reprocessed state after weathering (REP).

		Crystallinity percentages (%)			
		PP/WF10		PP/WF30	
1st heating ramp	INIT	46.0%	±0.9%	42.3%	±4.2%
	NAT	45.5%	±0.1%	37.8%	±2.0%
	REP	44.2%	±1.6%	42.2%	±2.0%
2nd heating ramp	INIT	50.7%	±0.5%	46.9%	±3.1%
	NAT	43.6%	±3.1%	43.4%	±2.3%
	REP	46.9%	±0.2%	47.0%	±2.0%

3.2.3. Conclusion

To sum up the results obtained from static mechanical tests, the addition of wood flour reduces the ductility of PP and reduces the sensitivity against degradation by natural weathering and reprocessing thanks to the antioxidant role of lignin [22,23]. A "regeneration" tendency can be observed with the reprocessing as it enables to recover a part of tensile ultimate strength, elongation at break and impact strength. The same tendencies were previously obtained for artificial weathered and reprocessed samples [19]. A competition between chain scission and chain recombination mechanisms and a transfer of degraded chains from amorphous phases to crystalline phases are suggested [19,25,26]. To complement these hypotheses, the polymer microstructure is investigated further on.

3.3. Evolution of the polymer microstructure

3.3.1. Crystallinity variations

The crystallinity percentages are calculated from the melting enthalpy on the first and the second heating ramp (Table 3). As the melting enthalpy measured during the first heating ramp is related to the initial crystallinity, it depends on the thermal background of the sample i.e. the ageing and/or reprocessing step.

On the first ramp, considering the large scattering no significant evolution could be revealed between PP/WF10 and PP/WF30 at the different stages with equivalent crystallinity percentages in the range of 42%–46%. These results show that the matrix crystallinity does not have a significant impact on the mechanical properties.

On the second ramp, similar results are obtained between PP/WF10 and PP/WF30 at the initial state. Nevertheless the natural weathering induces a slight decrease of crystallinity for both PP/WF composites. This decrease is presumably caused by an increased number of impureties in the material which can be deposited during the outdoor exposure such as dust or moisture. The presence of molecules that are smaller and more defective (because of foreign groups like carbonyl and hydroperoxides) is also suggested [33]. Then the REP samples recovered crystallinity values compared to NAT samples.

If comparing to the effect of an artificial weathering [19], an inverse tendency was found. The crystallinity ratio increases after artificial weathering because of the crystallisation of shorter chains. The first heating ramp revealed that the REP stage reached the initial value matching with observations from mechanical results. On the contrary, the second heating ramp showed that crystallinity values are the same after the REP stage leading to conclude the reprocessing did not influence significantly the crystallisation. Similarly to this present study, the artificial weathering study shows that the changes in crystallinity do not impact significantly the mechanical properties.

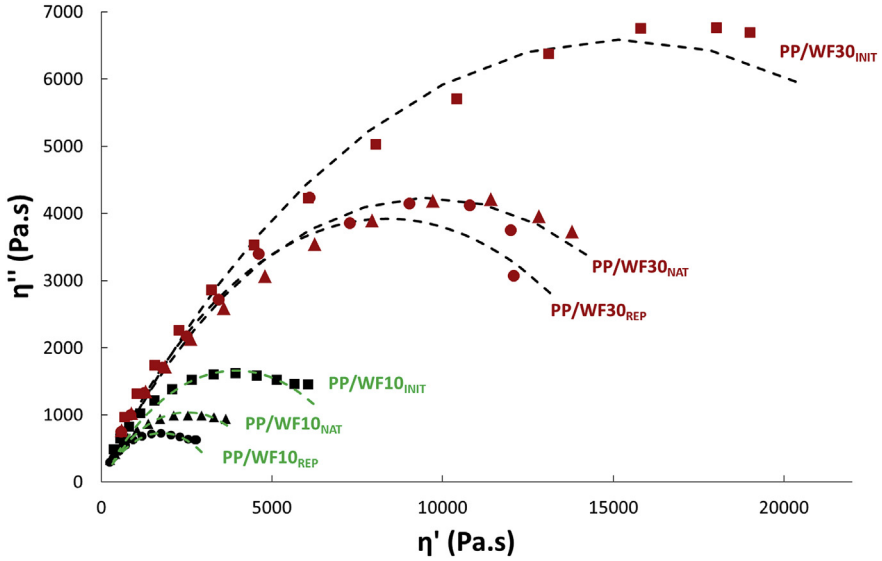


Fig. 6. Rheological results in complex plane diagrams with Cole-Cole model in dashed line of PP/WF10 (a) and PP/WF30 (b) at every stage(INIT, NAT, REP) with experimental data (in dots).

Table 4
Rheological parameters and SEC results for the PP/WF composites.

Materials		λ (s)[a]	α[b]	η_0 (Pa s)[c]	$\overline{Mn}$(g/mol)	$\overline{Mw}$(g/mol)	Ip = $\overline{Mw}/\overline{Mn}$
$PP/WF10_{INIT}$		1.06	0.49	7875	69 640 ± 2970	294 095 ± 32 067	4.2
$PP/WF10_{NAT}$	Exposed face	0.98	0.50	5023	25 185 ± 233	178 535 ± 6385	7.1
	Unexposed face				55 120 ± 3889	323 565 ± 3274	5.9
$PP/WF10_{REP}$		0.63	0.50	3548	38 280 ± 622	247 745 ± 5452	6.5
$PP/WF30_{INIT}$		3.23	0.48	30 512	55 070 ± 2249	281 055 ± 24 204	5.1
$PP/WF30_{NAT}$	Exposed face	1.87	0.47	19 170	31 025 ± 8987	259 490 ± 17 918	8.8
	Unexposed face				53 145 ± 1336	308 970 ± 13 718	5.8
$PP/WF30_{REP}$		1.44	0.44	16 734	46 235 ± 2355	273 720 ± 3974	8.9

[a] Relaxation time calculated from Cole-Cole model on experimental results at 180 °C.
[b] Distribution parameter of relaxation times from Cole-Cole model on experimental results at 180 °C.
[c] Newtonian viscosity calculated from Cole-Cole model on experimental results at 180 °C.

3.3.2. Viscosity and macromolecular weight variations

Rheological results are plotted in Fig. 6 using a Cole-Cole diagram representation (imaginary part of the complex viscosity η* as a function of its real counterpart) for PP/WF composites. PP/WF10 presents a progressive decrease of viscosity after natural weathering and then reprocessing related only to a chain scission mechanism. PP/WF30 has a higher viscosity because of its high wood content and shows also a decrease of viscosity after natural weathering and reprocessing.

In earlier studies [34,35] correlations between Cole-Cole results and degradation mechanisms during ageing for numerous polymers were evidenced. Thus a progressive drop of newtonian viscosity and a diminishing circular arc caused by a chain scission phenomenon is expected as reported by Verney [34]. Nevertheless, the addition of wood flour induces significants gaps between experimental data (in dots) and the Cole-Cole models (in dashed lines) meaning that wood particles may impact PP rheological behaviour.

In accordance with Havriliak and Negami equations [36], the relaxation time λ, the relaxation time dispersion α and the newtonian viscosity η_0 by extrapolation to low frequencies can be determined as developed in our previous study [19]. These

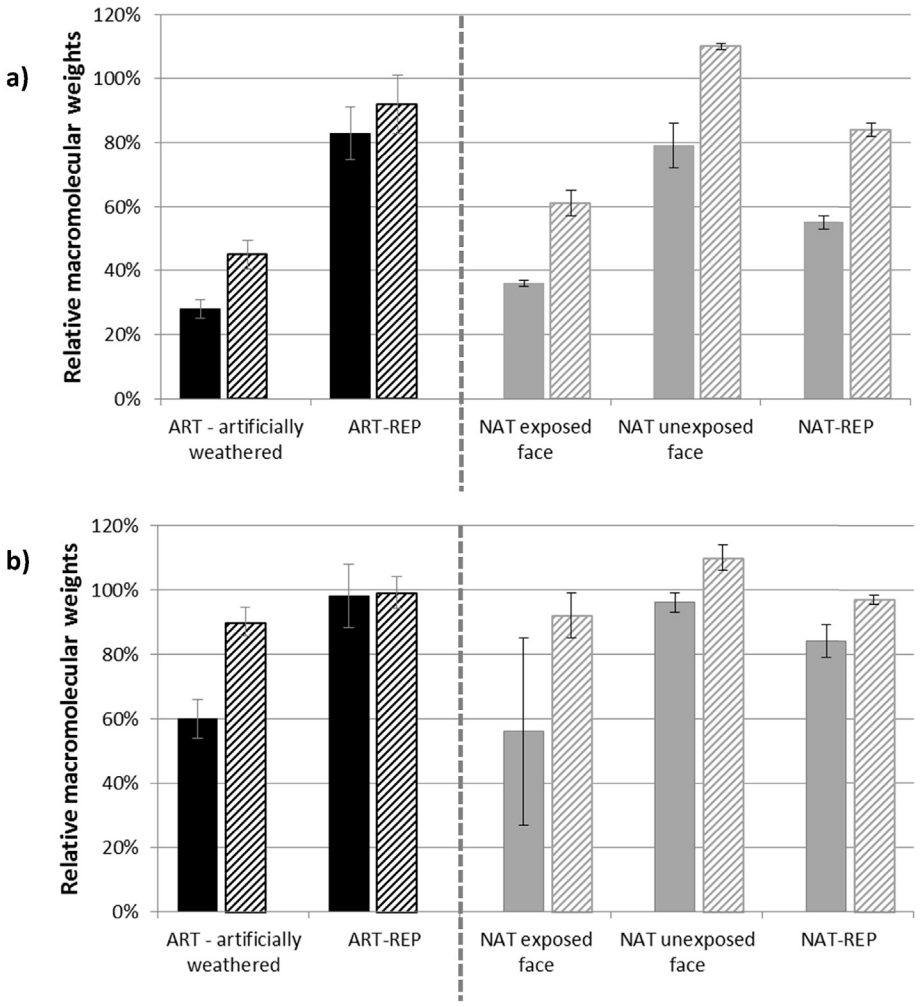


Fig. 7. Relative macromolecular weights for PP/WF10 (a) and PP/WF30 (b) compared to the initial state: Mn in plain bars and Mw in striped bars.

parameters are representative of the polymer mobility and the polymer chain length above melting temperature. Table 4 displays these parameters calculated with the Cole-Cole model as well as average molecular weights in number ($\overline{Mn}$) and in weight ($\overline{Mw}$) and polydispersity index ($Ip = \overline{Mw}/\overline{Mn}$) measured through SEC for the PP/WF composites. For PP/WF_{NAT} samples, both exposed and non-exposed surfaces were analyzed.

At the initial stage PP/WF30 exhibit a higher relaxation time λ than PP/WF10 because of the higher wood content restraining the polymer chain mobility (1.06 s for PP/WF10 and 3.23 s for PP/WF30). The newtonian viscosity η_0 is also superior for PP/WF30 and must be due to wood flour restraining chain mobility. Moreover, their respective chain weigths by weight and by number are very close meaning that wood flour does not impact significantly the PP matrix at the initial state. In the artificial weathering case, similar trends are observed at the initial state but values are different because of different processing conditions.

The relaxation time λ diminishes after natural weathering and reprocessing (from 1.06 s to 0.63 s for PP/WF10 and from 3.23 s to 1.44 s for PP/WF30) as chain mobility is improved by chain scissions. The distribution parameter α does not show a significant variation whatever the composites and stages. The newtonian viscosity η_0 shows a progressive decrease after every step as expected with chain scission phenomenon but remains higher for PP/WF30. This decrease in viscosity is about −55% for PP/WF10 and -45% for PP/WF30 evidencing that PP/WF30 is slightly less sensitive to degradation under these conditions. By comparing SEC data between exposed and unexposed surfaces, it can be highlighted that a stronger chain scission by photodegradation on the exposed surface occurs. SEC results after the REP stage show intermediate values meaning that the reprocessing has induced a mix of more or less degraded areas of the materials by grinding and injection moulding of the whole dog-bone samples. The polydispersity index increases with weathering and reprocessing. It can be induced by a chain scission phenomenon predominent on the chain extremities.

As concerns artificial weathering [19], similar degradations were observed after UV exposure with decreases in relaxation times, viscosities and macromolecular weights attributed to chain scission through photodegradation. Besides, the polydispersity indexes are superior for artificial weathering meaning that degradation is stronger at the chain ends under these conditions than under natural weathering.

The relative values of macromolecular weights are plotted in Fig. 7 for the two studies. The considered references are the values at the initial state. A complete recovery of the macromolecular weights is obtained after reprocessing in the case of artificial weathering certainly due to a recombination of PP chains. On the contrary, the reprocessing does not allow this recovery in our present study: macromolecular weight values after reprocessing are intermediate between values of the exposed and unexposed faces. It can be explained by a mixture of degraded and non-degraded chains with no recombination. As polydispersity

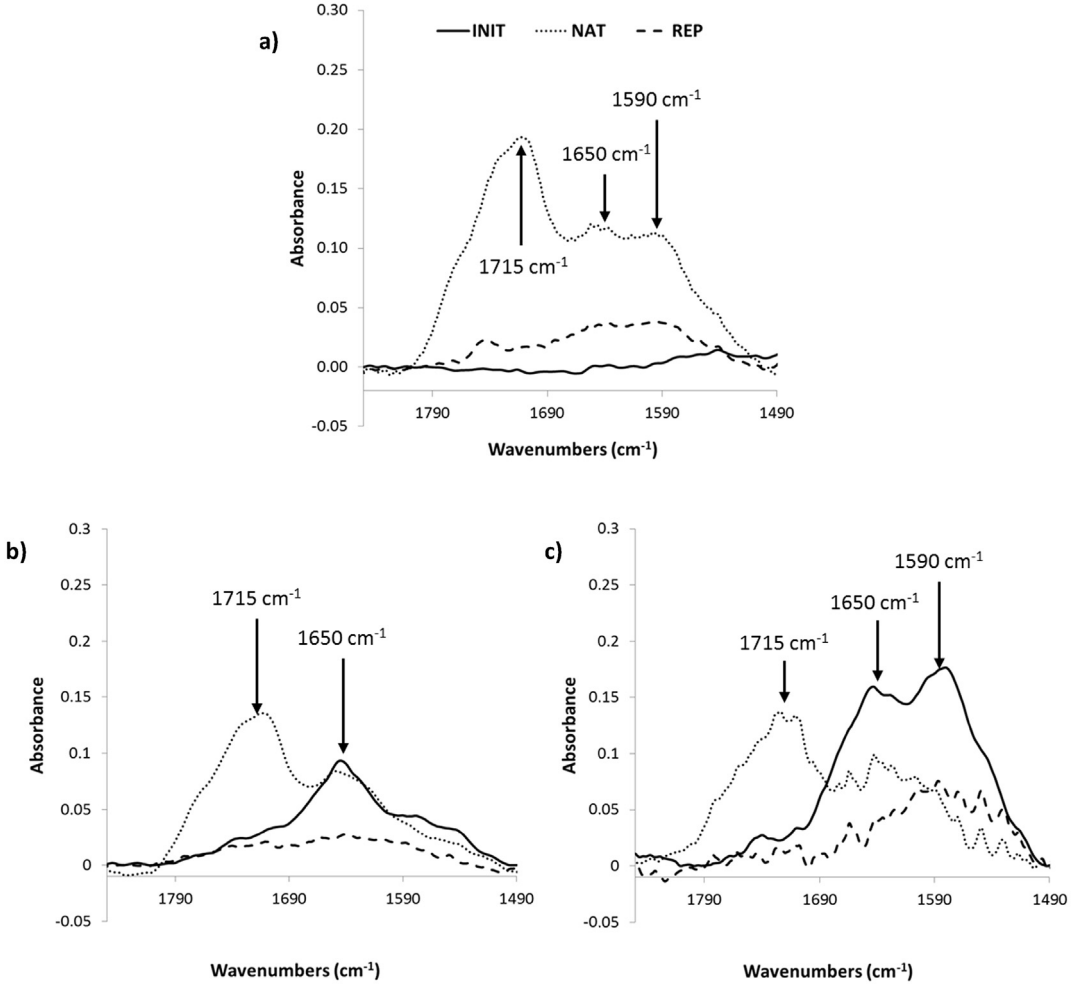


Fig. 8. Infrared spectrum of PP (a), PP/WF10 (b) and PP/WF30 (c) at the different stages (INIT, NAT and REP).

indexes were found to be different, variations between these two studies can be partly explained by differences in chain weight distribution.

3.3.3. Evolution of chemical structure

Infrared spectroscopy is used to determine structural and chemical changes of the studied materials after weathering and reprocessing. The present investigation is focused on the analysis of carbonyl and vinyl groups in the range of 1800 cm^{-1} to 1500 cm^{-1} [37]. Infrared spectra are presented in this range for PP and PP/WF composites and at each stage in Fig. 8.

Neat PP (Fig. 8a) presents three high degradation peaks after natural weathering exposure: the main one is located at 1715 cm^{-1} and corresponds to carboxylic acid whereas the remaining two attributed to 1650 cm^{-1} and 1590 cm^{-1})match with vinyl groups. These groups are typical of PP photodegradation [33,37]. After reprocessing, the spectrum returns to low absorbance values and shows that carbonyl and vinyl groups have disappeared from the sample surface.

At the initial state, PP/WF10 presents a 1650 cm^{-1} peak whereas PP/WF30 shows two higher peaks at 1650 cm^{-1} and 1590 cm^{-1}. These peaks correspond to C=C stretching in the lignin aromatic rings contained in wood flour. It is due to the presence of wood particles at the surface. Thus the addition of wood flour impacts surface chemical groups especially at high content such as at 30% wt. For both PP/WF composites, the weathering provokes the appearance of a high 1715 cm^{-1} peak and a lower peak at 1650 cm^{-1}. Respectively attributed to carbonyl groups and vinyl groups, these peaks can be related to both PP and lignin photodegradation and wood particles protrusion [21,33]. The PP/WF composite spectra shape does not differ much from the PP spectrum at the weathered state.

Concerning the effect of reprocessing, the disappearance of all degradation peaks can be observed. This can be attributed to the homogenization of the material through grinding and injection moulding as also observed in our previous study [19]. Indeed, the degraded chains from the sample skin and the non-degraded ones from the sample core are mixed together.

4. Conclusion

The aim of this work was to assess the influence of natural outdoor UV weathering on the potential of reprocessing of spruce wood flour reinforced PP composites (grinding-injection moulding cycles) with 10%wt and 30%wt wood content. Numerous experiments were carried out at the initial (INIT), naturally aged (NAT) and reprocessed (REP) stages.

The visual observation of the surfaces after weathering has shown a strong micro cracking phenomenon for neat PP and PP/WF composites. Moreover, the PP/WF composites have exhibited a surface bleaching and a wood particle protrusion which are more important with the higher wood content. After reprocessing, the neat PP became yellow while the PP/WF composites display the disappearance of the bleaching effect and a darker brown colour.

After natural weathering and reprocessing, the mechanical properties measured by tensile and impact tests have highlighted a "regeneration" phenomenon similarly to our previous study with artificial weathering: despite the mechanical degradation due to chain scission during photo-oxidation, the reprocessing step allows to recover the initial properties. Increasing wood content limits the material degradation and this can be explained by the antioxidant role of lignin.

DSC tests performed on PP/WF composites have evidenced a slight decrease in polymer crystallinity after natural weathering which is recovered after reprocessing. No specific correlation with the mechanical properties is observed.

Rheological tests have shown that the reprocessing step promotes this chain scission furthermore. SEC results disclosed that the reprocessing step consists mainly in mixing degraded chains and non-degraded ones, leading to an intermediate macromolecular weight values between the exposed and the unexposed face values. No recombination mechanism was detected contrary to our previous study.

Infrared spectroscopy analyses led to conclude that the photodegradation induces the formation of carbonyl and vinyl groups attributed to both wood flour and PP degradation. The reprocessing step induces the mixing and the dilution of the degraded chains into the material and the injection of smooth samples with a low wood content at the surface.

To resume, a regeneration mechanism was observed and is well correlated well previous results with artificial UV weathering. Although the one-year natural weathering is more detrimental on mechanical properties than the 14-days artificial weathering, similar trends in photodegradation and regeneration after reprocessing were highlighted. Through this comparison, the major conclusion in material evolution is that no polymer chain recombination was observed when the material is naturally weathered contrarily to artificial weathering. It is assumed that macromolecular weight distribution and presence of impurities from outdoor may explain this difference.

Acknowledgements

Authors are embedded to ADEME French organization for the financial support ENOLIBIO "ENd Of LIfe of BIOcomposites" (1101C0066).

References

[1] J.A. Youngquist, G.E. Myers, J.M. Muehl, A.M. Krzysik, C.M. Clemons, Composites from Recycled Wood and Plastics, Final Report for U.S. Environmental Protection Agency, Project #IAGDW-12934608-2, USDA, Forest Service, Forest Products Laboratory, Madison WI, 1993.

[2] K.B. Adhikary, S.P. Staiger, M.P. Staiger, Dimensional stability and mechanical behaviour of wood–plastic composites based on recycled and virgin high-density polyethylene (HDPE), Compos. Part B Eng. 39 (2008) 807–815, http://dx.doi.org/10.1016/j.compositesb.2007.10.005.

[3] L. Soccalingame, A. Bourmaud, D. Perrin, J.-C. Benezet, A. Bergeret, Reprocessing of wood flour reinforced polypropylene composites: impact of particle size and coupling agent on composite and particle properties, Polym. Degrad. Stab. 113 (2015) 72–85, http://dx.doi.org/10.1016/j.polymdegradstab.2015.01.020.

[4] G. Guerrica-Echevarria, J.I. Eguiazabal, J. Nazabal, Effects of processing conditions on the properties of unfilled and talc-filled polypropylene, Polym. Degrad. Stab. 53 (1996) 1–8, http://dx.doi.org/10.1016/0141-3910(96)00018-3.

[5] J.J. Balatinecz, M.M. Sain, The influence of recycling of wood fiber plastic composites, Macromol. Symp. 135 (1998) 167–173, http://dx.doi.org/10.1002/masy.19981350119.

[6] S.V. Canevarolo, Chain scission distribution function for polypropylene degradation during multiple extrusions, Polym. Degrad. Stab. 70 (2000) 71–76, http://dx.doi.org/10.1016/S0141-3910(00)00090-2.

[7] Q. Xiang, M. Xanthos, S. Mitra, S.H. Patel, J. Guo, Effects of melt processing on volatile emissions and structural/rheological changes of unstabilized polypropylene, Polym. Degrad. Stab. 77 (2002) 93–102, http://dx.doi.org/10.1016/S0141-3910(02)00083-6.

[8] M.H. Martins, M.A. De Paoli, Polypropylene compounding with post-consumer material: II. Processing, Polym. Degrad. Stab. 78 (2002) 491–495, http://dx.doi.org/10.1016/S0141-3910(02)00195-7.

[9] H.M. da Costa, V.D. Ramos, Marisa C.G. Rocha, Rheological properties of polypropylene during multiple extrusion, Polym. Test. 24 (2005) 86–93, http://dx.doi.org/10.1016/j.polymertesting.2004.06.006.

[10] C. Meran, O. Ozturk, M. Yuksel, Examination of the possibility of recycling and utilizing recycled polyethylene and polypropylene, Mater. Des. 29 (2008) 701–705, http://dx.doi.org/10.1016/j.matdes.2007.02.007.

[11] S. Kazemi-Najafi, M. Mostafazadeh-Marznaaki, M. Chaharmahali, M. Tajvidi, Effect of thermo-mechanical degradation of polypropylene on mechanical properties of wood–polypropylene composites, J. Compos. Mater. 43 (2009) 2543–2554, http://dx.doi.org/10.1177/0021998309345349.

[12] N. Bahlouli, D. Pessey, C. Raveyre, J. Guillet, S. Ahzi, A. Dahoun, J.M. Hiver, Recycling effects on the rheological and thermomechanical properties of polypropylene-based composites, Mater. Des. 33 (2012) 451–458, http://dx.doi.org/10.1016/j.matdes.2011.04.049.
[13] A. Bourmaud, C. Baley, Investigations on the recycling of hemp and sisal fiber reinforced polypropylene composites, Polym. Degrad. Stab. 92 (2007) 1034–1045, http://dx.doi.org/10.1016/j.polymdegradstab.2007.02.018.
[14] A. Bourmaud, A. Le Duigou, C. Baley, What is the technical and environmental interest in reusing a recycled polypropylene–hemp fibre composite? Polym. Degrad. Stab. 96 (2011) 1732–1739, http://dx.doi.org/10.1016/j.polymdegradstab.2011.08.003.
[15] L. Augier, G. Sperone, C. Vaca-Garcia, M.-E. Borredon, Influence of the wood fibre filler on the internal recycling of poly(vinyl chloride)-based composites, Polym. Degrad. Stab. 92 (2007) 1169–1176, http://dx.doi.org/10.1016/j.polymdegradstab.2007.04.010.
[16] A. Bourmaud, D. Akesson, J. Beaugrand, A. Le Duigou, M. Skrifvars, C. Baley, Recycling of L-Poly-(lactide)-Poly-(butylene-succinate)-flax biocomposite, Polym. Degrad. Stab. 128 (2016) 77–88, http://dx.doi.org/10.1016/j.polymdegradstab.2016.03.018.
[17] M.D.H. Beg, K.L. Pickering, Accelerated weathering of unbleached and bleached kraft wood fibre reinforced polypropylene composites, Polym. Degrad. Stab. 93 (2008) 1939–1946, http://dx.doi.org/10.1016/j.polymdegradstab.2008.06.012.
[18] W. Wang, M. Sain, P.A. Cooper, Hygrothermal weathering of rice hull/HDPE composites under extreme climatic conditions, Polym. Degrad. Stab. 90 (2005) 540–545, http://dx.doi.org/10.1016/j.polymdegradstab.2005.03.014.
[19] L. Soccalingame, D. Perrin, J.-C. Benezet, S. Mani, F. Coiffier, E. Richaud, A. Bergeret, Reprocessing of artificial UV-weathered wood flour reinforced polypropylene composites, Polym. Degrad. Stab. 120 (2015) 313–327, http://dx.doi.org/10.1016/j.polymdegradstab.2015.07.013.
[20] S.K. Najafi, Use of recycled plastics in wood plastic composites – a review, Waste Manag. 33 (2013) 1898–1905, http://dx.doi.org/10.1016/j.wasman.2013.05.017.
[21] L.M. Matuana, S. Jin, N.M. Stark, Ultraviolet weathering of HDPE/wood–flour composites coextruded with a clear HDPE cap layer, Polym. Degrad. Stab. 96 (2011) 97–106, http://dx.doi.org/10.1016/j.polymdegradstab.2010.10.003.
[22] Y. Peng, R. Liu, J. Cao, Y. Chen, Effects of UV weathering on surface properties of polypropylene composites reinforced with wood flour, lignin, and cellulose, Appl. Surf. Sci. 317 (2014) 385–392, http://dx.doi.org/10.1016/j.apsusc.2014.08.140.
[23] Y. Peng, R. Liu, J. Cao, Characterization of surface chemistry and crystallization behavior of polypropylene composites reinforced with wood flour, cellulose, and lignin during accelerated weathering, Appl. Surf. Sci. 332 (2015) 253–259, http://dx.doi.org/10.1016/j.apsusc.2015.01.147.
[24] H. Jia, H. Wang, W. Chen, The combination effect of hindered amine light stabilizers with UV absorbers on the radiation resistance of polypropylene, Radaition Phys. Chem. 76 (2007) 1179–1188, http://dx.doi.org/10.1016/j.radphyschem.2006.12.008.
[25] A. Jansson, K. Möller, T. Gevert, Degradation of post-consumer polypropylene materials exposed to simulated recycling—mechanical properties, Polym. Degrad. Stab. 82 (2003) 37–46, http://dx.doi.org/10.1016/S0141-3910(03)00160-5.
[26] S. Luzuriaga, J. Kovářová, I. Fortelný, Degradation of pre-aged polymers exposed to simulated recycling: properties and thermal stability, Polym. Degrad. Stab. 91 (2006) 1226–1232, http://dx.doi.org/10.1016/j.polymdegradstab.2005.09.004.
[27] L.H. Sperling, Introduction to Physical Polymer Science, fourth ed., John Wiley & Sons Inc, 2006, ISBN 9780471757115, p. 244.
[28] J. Laffargue, Etude et modélisation des instabilités du procédé de soufflage de gaine, PhD thesis in Material Science and Engineering, Ecole des Mines de Paris, Paris, 2003, p. 168.
[29] S. Havriliak, S. Negami, A complex plane representation of dielectric and mechanical relaxation processes in some polymers, Polymer 8 (1967) 161–210, http://dx.doi.org/10.1016/0032-3861(67)90021-3.
[30] L.M. Matuana, N.M. Stark, Surface chemistry changes of weathered HDPE/wood flour composites studied by XPS and FTIR spectroscopy, Polym. Degrad. Stab. 86 (2004) 1–9, http://dx.doi.org/10.1016/j.polymdegradstab.2003.11.002.
[31] K. Chaochanchaikul, K. Jayaraman, V. Rosarpitak, N. Sombatsompop, Influence of lignin content on photodegradation in wood/HDPE composites under UV weathering, BioResources 7 (2012) 38–55, 18pp.
[32] M. Muasher, M. Sain, The efficacy of photostabilizers on the color change of wood filled plastic composites, Polym. Degrad. Stab. 91 (2006) 1156–1165, http://dx.doi.org/10.1016/j.polymdegradstab.2005.06.024.
[33] S. Butylina, M. Hyvärinen, T. Kärki, A study of surface changes of wood-polypropylene composites as the result of exterior weathering, Polym. Degrad. Stab. 97 (2012) 337–345, http://dx.doi.org/10.1016/j.polymdegradstab.2011.12.014.
[34] V. Verney, Rheology, Oxidation and Polymer Aging, vol. 13, Rhéologie, 2008.
[35] H. Askanian, Etude de la durabilité de matériaux respectueux de l'environnement/biocomposites, PhD thesis in Chemistry – Physics, Université Blaise Pascal, Clermont-Ferrand, 2011, p. 164.
[36] S. Havriliak, S. Negami, A complex plane representation of dielectric and mechanical relaxation processes in some polymers, Polymer 8 (1967) 161–210, http://dx.doi.org/10.1016/0032-3861(67)90021-3.
[37] J.S. Fabiyi, A.G. McDonald, M.P. Wolcott, P.R. Griffiths, Wood plastic composites weathering: visual appearance and chemical changes, Polym. Degrad. Stab. 93 (2008) 1405–1414, http://dx.doi.org/10.1016/j.polymdegradstab.2008.05.024.